

Journal Pre-proof

Self-crosslinked chitosan/dialdehyde xanthan gum blended hypromellose hydrogel for the controlled delivery of ampicillin, minocycline and rifampicin

Fahanwi Asabuwa Ngwabebhoh, Oyunchimeg Zandraa, Rahul Patwa, Nabanita Saha, Zdenka Capáková, Petr Saha



PII: S0141-8130(20)35025-X

DOI: <https://doi.org/10.1016/j.ijbiomac.2020.11.100>

Reference: BIOMAC 17263

To appear in: *International Journal of Biological Macromolecules*

Received date: 3 September 2020

Revised date: 12 November 2020

Accepted date: 13 November 2020

Please cite this article as: F.A. Ngwabebhoh, O. Zandraa, R. Patwa, et al., Self-crosslinked chitosan/dialdehyde xanthan gum blended hypromellose hydrogel for the controlled delivery of ampicillin, minocycline and rifampicin, *International Journal of Biological Macromolecules* (2018), <https://doi.org/10.1016/j.ijbiomac.2020.11.100>

This is a PDF file of an article that has undergone enhancements after acceptance, such as the addition of a cover page and metadata, and formatting for readability, but it is not yet the definitive version of record. This version will undergo additional copyediting, typesetting and review before it is published in its final form, but we are providing this version to give early visibility of the article. Please note that, during the production process, errors may be discovered which could affect the content, and all legal disclaimers that apply to the journal pertain.

Research Article**Self-crosslinked chitosan/dialdehyde xanthan gum blended hypromellose hydrogel for the controlled delivery of ampicillin, minocycline and rifampicin****Fahanwi Asabuwa Ngwabebhoh, Oyunchimeg Zandraa, Rahul Patwa, Nabanita Saha, Zdenka Capáková, Petr Saha***Centre of Polymer Systems, University Institute, Tomas Bata University in Zlin, Tr. T. Bati 5678, 76001, Zlin, Czech Republic***Abstract**

The design of improved biopolymeric based hydrogel materials with high load-capacity to serve as biocompatible drug carriers is a challenging task with vital implications in health sciences. In this work, chitosan crosslinked dialdehyde xanthan gum interpenetrated hydroxypropyl methylcellulose gels were developed for the controlled delivery of different antibiotic drugs including ampicillin, minocycline and rifampicin. The prepared hydrogel scaffolds were characterized by rheology method, FTIR, SEM, TGA and compression analysis. In addition, gelation kinetics, swelling, *in vitro* degradation and drug release rate were studied under simulated gastrointestinal fluid conditions of pH 2.0 and 7.4 at 37 °C. Results demonstrated the gel composition and structure affected drug release kinetics. The release study showed more than 50% cumulative release within 24 h for all investigated antibiotic drugs. *In vitro* cell cytocompatibility using mouse embryonic fibroblast cell lines depicted $\geq 80\%$ cell viability, indicating the gels are non-toxic. Finally, the antibacterial activity of loaded gels was evaluated against Gram-negative and positive bacteria (*Escherichia coli*, *Staphylococcus aureus* and *Klebsiella pneumonia*), which correlated well with swelling and drug release results. Overall, the present study demonstrated that the produced hydrogel scaffolds serves as promising material for controlled antibiotic delivery towards microbial growth inhibition.

Keywords: Hydrogel, Biopolymers, Antibacterial activity, Antibiotic drug delivery

Corresponding authors:

E-mail address: F.A. Ngwabebhoh (asabuwa@utb.cz/asabuwa.nf@gmail.com)N. Saha (nabanita@utb.cz)

1. Introduction

Antibiotics are well known to be used for systemic therapy via parenteral, enteral and topical administration for bacterial infections [1]. However owing to short half-life *in vivo*, most antibiotics and conventional drug delivery systems limit the ideal pharmacokinetic profile of the drugs thereby displaying a level of toxicity and narrow therapeutic effect at targeted infected sites [2, 3]. Therefore, an urgent need for the design and development of formulations that can provide sustained and controlled release for this class of drugs is of great research interest. For this purpose, several drug delivery systems based on different polymeric materials have been reported over the years for the entrapment of antimicrobial drugs with efforts towards improving sustained release properties [4-5]. Recently, biopolymeric hydrogel systems have been widely studied and applied in pharmaceuticals and biomedicine as suitable drug carriers [6]. Hydrogels as defined are three-dimensional physically or chemically crosslinked hydrophilic polymeric networks that can hold large quantity of water or biological fluids [7-9]. This class of 3D polymeric structured materials have been widely applied as drug delivery systems and tissue regeneration scaffolds due to their high biocompatibility, tuneable mechanical properties and porous structure [10]. In recent years, hydrogels prepared from natural polymers have been extensively explored via different physical and covalent crosslinking techniques, producing biodegradable materials for used as drug carriers and cell growth scaffolds [11-13].

Over the years, natural polymers have demonstrated to be excellent candidates in the preparation of hydrogels attributed to their low cost, ready availability, good mechanical strength, outstanding biocompatibility, low toxicity and biodegradability [14, 15]. Amongst all, chitosan (CS) is one of several natural polymers widely used in the fabrication of hydrogels. This biopolymer mainly extracted from N-deacetylation of chitin has demonstrated a wide range of applications in biomedicine, attributed to its cytocompatibility and biodegradability, mucoadhesiveness and antibacterial activity [16]. Also, the active amino and hydroxyl functional groups on the polymer backbone provides great potential for different side group functionalization [17]. Xanthan gum (XG) on the other hand, is another natural polymer extracted from the bacteria *Xanthomonas campestris* with great research potential in drug delivery and tissue regeneration application [18]. This biopolymer in the presence of sodium periodate can be oxidized via C-C cleavage between C2-C3 bonds, resulting in the introduction of dialdehyde groups on the polymer backbone [19]. The

obtained oxidized polymer can efficiently react with amine groups via Schiff base reaction to form imide bonds. This technique has been widely applied in the preparation of dialdehyde biopolymers such as dialdehyde starch, dialdehyde sodium alginate, dialdehyde carboxymethyl cellulose and dialdehyde xanthan gum, which have been used as ideal crosslinking moieties to reinforce thermal, light barrier and mechanical properties of other materials [20-22].

Hydrogels in general are prepared from physical or covalent crosslinked polymer systems that can seldom satisfy the required properties of a drug delivery system due to the weak crosslinked network structures formed via partial inter/intra chain interactions [7]. In order to enhance the structural integrity of the crosslinked network assembly, the parent hydrogel systems are mixed with other polymers or derivatives. It has been reported that by blending a crosslinked system with different polymers can offer new structural materials with improved properties such as high swelling degree, good mechanical stability and porosity [23]. Hydroxypropyl methylcellulose (HC) also known as hypromellose is a hydrophilic cellulose derivative that has demonstrated great application in the control release of drug molecules [24]. This polymer has been approved by FDA as non-toxic to human body and has demonstrated to be a flexible incorporating additive into hydrogel systems by enhancing inter/intra-molecular and hydrophobic interactions in the blend system [25]. So far, the combination HC with a self-crosslinked hydrogel system composed of chitosan and dialdehyde xanthan gum for drug delivery applications has not yet been studied. Considering the numerous investigations available on hydrogel scaffolds for drug delivery systems, it is still imperative to develop new hydrogel systems as drug carriers with good drug loading efficiency, drug stability, sustain control release, biocompatibility and biodegradability.

Herein, a covalent crosslinking method by Schiff base reaction was employed to prepare biocompatible hydrogel scaffolds from naturally derived chitosan, xanthan gum and cellulose derivative. The mechanism of crosslinking was attributed to Schiff base reaction between amino and aldehyde groups of CS and oxidized XG interpenetrated with HC. The main aim of this study was to investigate the potential of the prepared hydrogel as an antibiotic drug carrier with sustain control release properties. To this aim, three different antibiotic drugs including ampicillin, minocycline and rifampicin that are very effective towards pathogenic bacteria were investigated. Primarily, characterization of the prepared hydrogel scaffolds was performed and their mechanical properties established via rheological and compression

analysis. The release kinetics of the different antibiotic drugs was explored and the antibacterial activity of the drug-loaded hydrogels established.

2. Experimental section

2.1. Materials

Chitosan (CS) high molecular weight (Mwt 310 - 375 kDa, degree of deacetylation 75–85%), xanthan gum (XG), hydroxypropyl methylcellulose (HC, also known as hypromellose), absolute ethanol (EtOH, $\geq 99\%$ purity), ethylene glycol, copper sulphate pentahydrate ($\text{CuSO}_4 \cdot 5\text{H}_2\text{O}$), sodium hydroxide (NaOH), phenolphthalein, hydrochloric acid (HCl, 37% purity) and sulphuric acid (H_2SO_4 , $\geq 95\%$ purity) were obtained from Sigma-Aldrich and used as received. Sodium periodate (NaIO_4) was supplied by Pentachemicals Ltd. Ampicillin trihydrate (AT, 97-99% purity), minocycline hydrochloride (MH, $\geq 98\%$ purity) and rifampicin (RC, $\geq 97\%$ purity) as the model antibiotic drugs were purchased from Sigma Aldrich. All chemicals were used without further purification and distilled water (dH_2O) was used for the preparation of solutions.

2.2. Preparation of oxidized xanthan gum

Dialdehyde xanthan gum (DA-XG) was prepared similar to previously described procedure [19, 26] with slight moderation. In brief, 2 g of XG was dissolved in 200 mL of dH_2O at 60 °C and once completely dissolved, the solution was allowed to cooled down to 40 °C. Under stirring, 20 mL of 0.096 g/mL NaIO_4 solution was added to dissolved XG and the pH of the mixture adjusted to pH 5 using 1M H_2SO_4 . The pH of the mixture was maintained at pH 5 under continuous stirring in the dark for 4-6 h. The reaction was stopped with 1 mL ethylene glycol and the oxidized XG mixture dialysed for 2 days to neutral pH using a dialysis bag of mwt cut-off 12 kDa. The purified sample was freeze dried producing white powder of DA-XG. The obtained dried DA-XG was then stored in a desiccator for further use.

The degree of oxidization of XG was further evaluated by titration following an alkali consumption quantitative method as previously described [27, 28]. 0.2 g of DA-XG was weighed and transferred into a 200 mL flat bottom flask containing 10 mL of 0.2M NaOH solution. The mixture was gently stirred in a water bath at 70 ± 3 °C for 3-5 min to completely dissolve the sample followed by immediate cooling under running tap water. 10 mL of 0.2M H_2SO_4 and 50 mL of dH_2O was then added to the mixture. Under continuous stirring, 3-5 drops 0.2 % w/v of phenolphthalein was added and the solution titrated against 0.2M NaOH to

reach a stable pink colour, indicating the endpoint of the titration. The percentage of the dialdehyde groups was then calculated using the equation below:

$$\%CHO = \frac{[V_{oxidized} - V_{control}] \times C_{NaOH}}{8 \times \frac{m}{MM}} \times 100 \quad (1)$$

Where, $V_{oxidized}$ and $V_{control}$ (mL) are the volumes of NaOH used to reach the endpoint during titration, respectively. C_{NaOH} is the concentration of NaOH in molarity, m is the dry weight of XG (g) used and MM is the approximate molecular weight (934 g/mol) of the repeating units of XG.

2.3. Fabrication of gels

A known amount of CS was dissolved in 0.2 %w/v acetic acid overnight and the solution adjusted to pH 5.5 using 0.1M NaOH. Different concentrations (0.5, 1.0, and 2.0 %w/v) of HC were dissolved in PBS and added to CS solution. Varying amounts of DA-XG were dissolved in PBS under heating and stirring. The dissolved DA-XG solutions were then added separately into prepared CS/HC mixtures and homogenized. According to literature, the optimal formation of imine (Schiff base) bonds is achievable at pH in the range of 5-6 [29]. However, imide bonds formed at this pH are less stable as compared to imines in basic pH 8-9. Considering the possible precipitation of dissolved chitosan in basic medium, the pH of the mixtures in the present study were initially maintained at pH 5.5 for optimal crosslinking. Followed by slowly adjusting the mixtures to basic pH 8-9 using 0.1M NaOH, producing less reversible and more stable imine (Schiff base) bonds gel network. The obtained gels were washed severally with distilled water to remove unreacted components, frozen at -80 °C and freeze dried in a lyophilizer. The obtained dried samples were then stored in a desiccator for further analysis and application. The formulation composition of the different gels is presented in **Table 1**.

Table 1
Compositions of prepared gels.

Samples	CS (%w/v)	DA-XG (%w/v)	HC (%w/v)
CX1	0.50	0.25	/
CX2	0.50	0.50	/
CXH1	0.50	0.50	0.50
CXH2	0.50	0.50	1.00
CXH3	0.50	0.50	2.00

2.4. Gelation, gel fraction and swelling analysis

Gelation as a function of time was investigated via the inverted tube test method as described previously [30, 31]. 1 mL of the prepared different gel solutions were transferred into 1.5 mL vials and allowed to solidify. The sol-gel transition time of the gel samples was achieved by inverting the vials every minute. Considering the test vials containing the solutions are titled and a deformation flow occurs, this is defined as a sol phase while if no flow occurs, it is described as a gel phase. Thus, the time at which a gel mixture did not flow once inverted was recorded as its gelation time.

Gel fraction of the prepared hydrogels was also determined as previously reported [32] with slight modification. A known weight (G_s) of freeze-dried hydrogel sample was immersed in dH₂O for a period 2 days at room temperature to extract unreacted reactants. The hydrogels were then removed, washed severally with dH₂O and dried to constant weight (G_F) in an oven at 60 °C. The gel fraction percentage ($GF\%$) was then determined using the equation: $GF\% = (G_F / G_o) \times 100$.

The swelling capacity of the gels was measured by immersing the lyophilized dried weighted samples in PBS (pH 7.4) at 37 °C for 24 h to reach equilibrium swelling. The samples were removed from the swelling phase, blotted with filter paper to extract excess water and weighed. The average value after triplicate readings was recorded and the equilibrium swelling percentages ($ES\%$) calculated using the equation below:

$$ES\% = \frac{W_F - W_O}{W_O} \times 100 \quad (2)$$

Where, W_F is the weight of the swollen gels after 24 h and W_O is the initial dry weight of the lyophilized gel samples.

2.5. Characterization techniques

Fourier transform infrared (FTIR) spectra of the prepared hydrogels was recorded using a Nicolet iS5 (Thermo Scientific, USA), scanned at a resolution of 4.0 cm⁻¹ in the range of 4000–400 cm⁻¹. The surface morphology of the hydrogels was observed by scanning electron microscopy (SEM) using a bench-top PhenomTM Pro microscope operating at 10 kV. The crystallinity index of the samples was analysed by a high-resolution Mini FlexTM 600 X-ray diffractometer (Rigaku, Japan). Thermogravimetric analysis was carried out using a TA

instrument Q50 V20.13 Build 39 thermogravimetric analyser at a heating rate of 20 °C/min from 25 to 500 °C under a nitrogen flow rate of 60 mL/min. To characterize the mechanical properties of the hydrogels, unconfined compressive tests were conducted at 25 °C under a static load of 5 kg and crosshead speed of 1 mm/min using a Testometric MT350-5CT (Labomachine, Czech Republic). The swollen hydrogel samples were cut into cylindrical shapes and compressed to 90% in order to measure the compressive modulus.

2.6. Rheology study

A rotational rheometer (Anton Paar MCR 502) with parallel plate geometry of 25 mm diameter was used to measure rheological parameters at 25 °C. A frequency sweep study was performed by varying the angular frequency from 0.1 to 100 rad/s at a constant amplitude of 1%. The storage modulus (G') and loss modulus (G'') were measured for the prepared hydrogels.

2.7. Drug loading in gels and loading efficiency

The drug loaded gels were prepared following similar protocol as the gel preparation. In brief, 1 mL from 1 mg/mL stock solution of the different single drugs (AT, MH and RC) were mixed with same amounts of dissolved HC and added to separate vials containing CS solution. DA-XG solution was subsequently added to the mixture and the pH adjusted for optimal crosslinking and stable imine formation. The obtained drug loaded samples were then freeze-dried followed by determination of the drug loading efficiency (DLE). In order to evaluate the DLE, weighed amounts of the different drug loaded gel samples were separately re-immersed each in 10 mL H₂O:methanol (ratio 7:3) solutions and allowed to swell for an hour. The swollen drug loaded gels were then crushed and mixture solution transferred to separate 2 mL test vials. The samples were centrifuged at 14000 rpm using a micro-spin centrifuge and the supernatant collected to determine the drug loading efficiency following absorbance readings on a UV-Vis single beam spectrophotometer (Model I-290) at 325, 350 and 475 nm for AL, MH and RC, respectively. Using prepared standard calibration curves for the different drugs, the DLE percentages (%) were calculated following the equation below:

$$\text{DLE}\% = \frac{\text{Total conc. of drug added} - \text{Conc. of drug in supernatant}}{\text{Total conc. of drug added}} \times 100 \quad (3)$$

2.8. *In vitro* release and drug release kinetics

The *in vitro* release of AT, MH, and RC drugs from CXH gel was studied in simulated gastrointestinal conditions. In the present study, PBS simulated gastric fluid (SGF) and simulated intestinal fluid (SIF) of pH 2.0 and 7.4, respectively, were used and the release studies performed in a shaking water bath at 100 rpm and temperature 37 °C [33]. In brief, samples were weighed and immersed in 100 mL of release media and at predetermined time intervals, 1 mL of release medium was collected and replaced with same amount of fresh PBS solution. The amount of drug released was then analysed spectrophotometrically using a UV-Vis single beam spectrophotometer (Model I-290) at 325, 350 and 475 nm for AT, MH and RC, respectively. Absorbance readings for MH and RC were performed directly, while that of AT was conducted after complexation with CuSO₄ (stock concentration 1mg/mL) following a 1:5 mixing volume ratio. Before absorbance readings, the complexed samples were kept for 25 minutes as described previously [34] with slight modification. The amount of the different antibiotic drugs released were determined from their calibration curves and the cumulative drug release percentages (CDR%) were determined by $(D_t/D_o) \times 100$, where, D_t is the total amount of drug released at time t and D_o is the initial amount of drug in the gels. In order to better describe the drug release mechanism, the release data for the various investigated drugs from CXH gel was further evaluated by computing and fitting the experimental data to Korsmeyer-Peppas kinetic model (Eq. 4) [35].

$$\frac{M_t}{M_\infty} = K_{KP} \times t^n \quad (4)$$

Where, M_t is the amount of drug released at time t , M_∞ is the amount of drug released as time approaches infinity and K_{KP} is the constant related to drug release that incorporate the structural and geometric properties based on the drug form. When Eq. 4 is converted to a logarithmic equation, the slope n that indicates the drug release mechanism can be determined by plotting the logarithm of release rate versus the logarithm of time. Where calculated $n \leq 0.5$ indicates the drug release is controlled by Fickian diffusion, $n \geq 1.0$ suggests a non-Fickian diffusion, $0.5 < n < 1.0$ describes an anomalous process, $n = 0.5$ a case I and $n = 1.0$ attributes to a case II transport process [36, 37].

2.9. *In vitro* cytocompatibility and degradation

The cytotoxicity of CXH gels was evaluated using ATCC-formulated Dulbecco's Modified Eagle's (DMEM) medium (Biosera, France) containing 10% of calf serum and 100 U/mL penicillin/streptomycin (Biosera, France) as the culture medium. The gels' extract was homogeneously mixed with the culture medium and used within 24 h. All tests were conducted in triplicates. The mouse embryonic fibroblast cells (ECACC 93061524, England) were seeded to pre-incubated microtitration test plate dishes (TPP, Switzerland) at a concentration of 1×10^5 cells/mL. The cell viability of the gels was then determined using 3-(4,5-dimethyl) thiazol-2-yl-2,5-dimethyl tetrazolium bromide (MTT) cell proliferation assay kit (Duchefa Biochemie, Netherlands). The absorbance of the solutions was read by a photometer at 570 nm wavelength. The cell viability results of the gels are presented in comparison to cells cultivated in medium without the extracts of tested samples.

In vitro degradation of the gels was performed following weight loss in PBS pH 7.4 aqueous solution during a period of 30 days similar to a previously reported protocol [38] with slight modification. Initially, weighted amounts (W_o) of lyophilized CXH gel samples were immersed in 50 mL PBS and incubated under mild shaking of 100 rpm in an oven at 37 °C. At different time intervals, the gel samples were removed from the PBS solution, gently blotted with tissue paper and weighed (W_d). Readings were performed in triplicates and the average value recorded. The weight loss percentage (WL%) was determined from $((W_o - W_d)/W_o) \times 100$.

2.10. Antibacterial study

Antibacterial activity of antibiotic drug loaded gels (CXH-AT, CXH-MH and CXH-RC) was assessed against *Escherichia coli* (CCM 4517), *Staphylococcus aureus* (CCM 4516), and *Klebsiella pneumonia* (CCM 4415) using agar disc diffusion test. A 100 μ L aliquot of each bacterial stock of approximate concentration 12×10^8 cells/mL was uniformly spread on a tryptone soya agar plate and the disc shape loaded gel samples (bulk drug concentration of 1 mg/mL and diameter = 6 mm) were placed on top of the plates. The plates were then incubated at 37 °C for 18 h and the inhibition zones measured. Control samples separately containing AT, MH and RC were prepared by dropping 20 μ L of 1 mg/mL drug stock solution onto sterilized filter paper of 6 mm diameter.

2.11. Statistical analysis

Results are displayed as Mean \pm Standard error of mean. OriginLab software version 9.0 was used for statistical analysis. The experimental data from all the investigations were analysed using analysis of variance (ANOVA). A value of $p < 0.05$ was determined as statistically significant.

3. Results and discussion

3.1. Synthesis of gels

Periodate oxidation has been widely utilized in the preparation of biopolymeric dialdehydes such as dialdehyde starch and dialdehyde cellulose via selective cleavage of C-C bonds between vicinal hydroxyl groups of anhydrous D-glucopyranose residues, producing a ring-opened structure containing two aldehyde groups [27]. According to this chemical modification technique, a large number of aldehyde groups (CHO) are introduced into polysaccharides backbone chains that can further react with ϵ -amino groups of other polymers via Schiff base reaction [39]. In the present study, pristine XG was oxidized in the presence of sodium periodate to yield the corresponding C2-C3 oxidized dialdehyde product (OXG). The chemical reaction of the formation of OXG via periodate oxidation of XG is given in **Fig. 1a**. Specifically, the reaction of XG with periodate occurs mainly by scission of C2-C3 glucosidic bonds, giving rise to two aldehyde groups (CHO) [40, 41]. The percentage content of CHO in OXG was calculated as $35.08 \pm 0.53\%$, which is similar to the results obtained by Guo et al. [19]. This indicated that aldehyde groups were successfully introduced in XG structural backbone. Following the results obtained from high-performance liquid chromatography (HPLC) analysis, the molar mass of pristine XG was $156,863 \pm 249$ g/mol, which on periodate oxidation decreased to $117,749 \pm 365$ g/mol. This reduction may be attributed to the opening of the pyranose ring structure and depolymerisation of XG.

According to the present research study, different CS–OXG crosslinked samples were prepared by varying the concentration of OXG forming hydrogels (CX) of varying crosslink densities. The crosslinking process was achieved by Schiff's base reaction between ϵ -amino groups ($-\text{NH}_2$) of chitosan and the introduced aldehyde of OXG forming imine bonds as shown in **Fig. 1b** [42]. In order to improve hydrophilicity and mechanical stability, HC was incorporated into the crosslinked structure to produce interpenetrated hydrogels (CXH). Various hydrogel samples were prepared by varying HC concentrations and the properties of

the obtained CXH gels compared to CX as control. The viscosities of the CXH hydrogels were observed to increase as the ratio of HC increased.

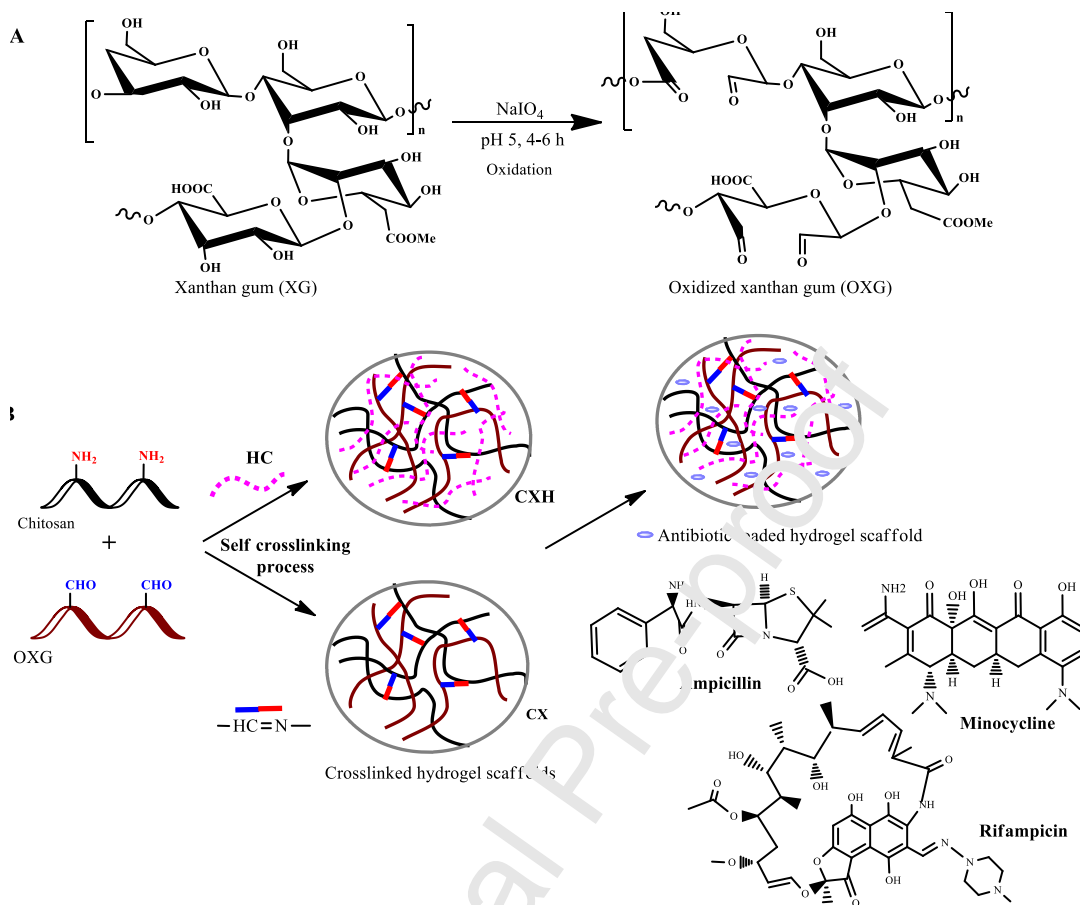


Fig. 1. Reaction scheme to show the preparation of a) oxidized xanthan gum and b) the different gel scaffolds (CX and CXH). The inset chemical structures relates to the different antibiotic drugs loaded in the hydrogels.

3.2. Gelation time, gel fraction and swelling analysis

Gelation rates of the hydrogel scaffolds containing different amount of OXG and HC were monitored at 37 °C and the results given in **Fig. 2a**. When CS and OXG solutions were mixed to form CX scaffolds, gelation occurred within 10 min and decreased to 6 min by increasing the crosslinking density using higher amounts of OXG. For CXH hydrogels, the addition of HC greatly increased the gelation time compared to prepared CX gels. However, a decrease from 47 to 30 min with increasing the content of HC was observed. This decrease in gelation time with increase in HC content is attributed to the increase in viscosity of the mixture medium as HC amount increases. Overall it was obvious that the incorporation of HC into the hydrogel systems significantly increased the gelation time and thus aided in the formation of more homogenous hydrogel systems.

Fig. 2b displays the gel fraction percentages of the prepared hydrogels. The gel fraction of the CX hydrogels increases from 86.41 to 90.26% attributed to the increase in the ratio of OXG, which intend increased crosslinking density. While CXH samples depicted a gel fraction decreased from 80.67 to 71.38% by increasing the amount of HC. This decrease in gel fraction ratio may be attributed to the hydrophilicity of HC, which increase high water absorbing affinity and possible leaching of HC polymer chains from the gel network.

Swelling properties are of vital importance for drug release and tissue engineering application [33]. It can be assumed that the swelling behaviour of the hydrogels mainly depends upon the different functional groups present on the backbone of the polymers. This promote hydrophilic-hydrophobic interactions as well as protonation or ionization thereby causing relaxation of polymeric matrix and network structure. In the present study, the swelling capability of the prepared hydrogels were investigated at different pH of 3.5, 5.5, 7.5 and 9.5. Results showed that highest swelling dynamics was achieved in acidic pH compared basic pH medium. Such behaviour may be attributed to the protonation of functional groups in CX and CXH hydrogels at acidic medium and deprotonation in basic environment. **Fig. 2c** shows the equilibrium swelling ratio of CX and CXH hydrogels in PBS at 37 °C during 24 h. It is observed that CXH hydrogels possessed higher swelling ratio than CX samples. This may be related to the higher number of hydrophilic groups, such as hydroxyl, carboxyl and amino groups, which contributed to the increase in water absorption [43]. However, since CS is non-water soluble, HC may occupy more portion of space in the porous structure and under aqueous conditions, CXH hydrogel will exhibit significantly higher and more stable swelling rates than CX. At acidic pH 3.5, the primary amino (NH_2) and hydroxyl (OH) groups of the polymers are protonated by hydrogen ions to form NH_3^+ and OH^+ groups that in tend enhances the uptake of water [44]. While at high pH 9.5, most of the swelling in the hydrogel is driven by deprotonated OH^- and to a lesser extent hydrogen bond interaction. The effect HC concentration also plays a great role on the swelling behaviour of the hydrogels as observed in **Fig. 2c** and **d** depicting swelling of the hydrogels increased on increasing the concentration of HC from 0.5 to 2% w/v. The hydrogels with high HC content exhibited highest swelling ratio in comparison to formulations with low or no HC. This phenomena may be attributed to the hydrophilic nature of HC and to a lesser extent OXG due to the presence of o-acetyl and pyruvyl residues, which can be completely deprotonated at $\text{pH} > 6$. To sum up, CXH3 and CX2 (as control) were determined as the optimal hydrogel samples with highest swelling abilities and will be used for further analysis and experimental evaluations.

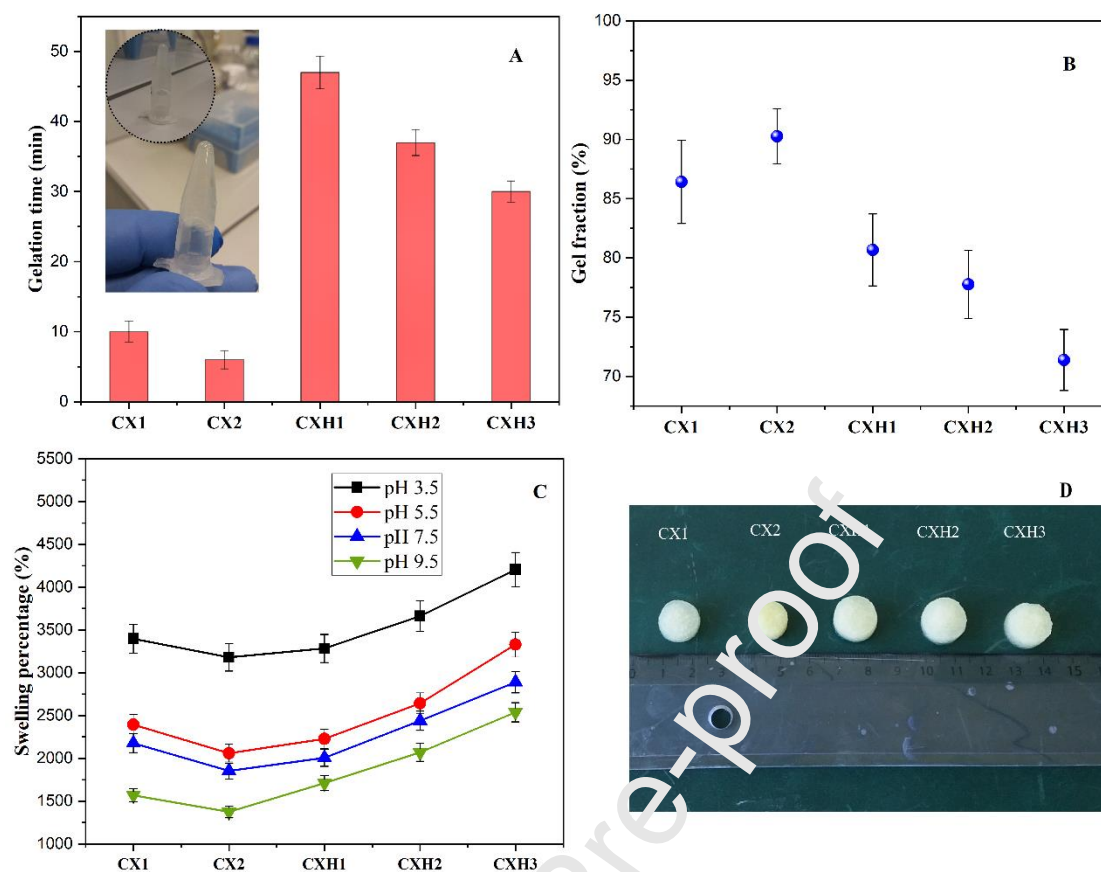


Fig. 2. a) Gelation time, b) gel fraction (inset image illustrate the gelation of gel in test vial), c) swelling capacity and d) photograph of swollen state of prepared gels.

3.3. Characterization of gels

3.3.1. FTIR analysis

FTIR spectra of XG, OXG and the developed hydrogels are presented in **Fig. 3**. The success of the periodate oxidation process was confirmed by comparing the FT-IR spectra of pristine XG and OXG. The peaks at $1220\text{-}1000\text{ cm}^{-1}$ (CO and C-O-C stretching vibrations), 1415 cm^{-1} (OH bending), 2920 cm^{-1} (CH vibrations) and $3600\text{-}3000\text{ cm}^{-1}$ (OH stretching vibration) were observed for both spectra. However, the appearance of the new peak at 1741 cm^{-1} is attributed to C=O stretching vibration related to the aldehyde groups of OXG. This indicated that the periodate oxidation process was successful. This observation is supported by similar results in a study by Malik et al. [43]. They reported the aldehyde absorbance peak of OXG via periodate oxidation related to the observed peak in the region of $1730\text{-}1720\text{ cm}^{-1}$. While the FTIR spectra of CX and CXH showed a typical broad band between $3000\text{ and }3600\text{ cm}^{-1}$ which is attributed to OH stretching vibrations may also overlaps with the stretching band of NH [45]. The peak in the range of $2920\text{ and }2880\text{ cm}^{-1}$ represents CH vibrations of methyl

and methylene (CH_2 and CH_3) groups. The other peaks observed includes 1643 cm^{-1} (amide I), 1595 cm^{-1} (NH_2 bending), 1413 cm^{-1} (stretching of OH bonds on the glucose molecule), 1150 cm^{-1} (stretching vibration of C-O-C) and finally the peak at 941 cm^{-1} that represents the in-phase vibrations from ether linkages attached to the peak at 1150 cm^{-1} [46, 47]. The stretching vibration of the imine group ($\text{C}=\text{N}$) that usually appears around 1640 cm^{-1} relates to the Schiff base reaction formed by reacting primary amines of chitosan and aldehyde groups of OXG was observed for both CX and CXH hydrogels. This confirms that the crosslinking between CS and OXG was successful. This is also supported by the disappearance of the new characteristic peak at around 1741 cm^{-1} in OXG related to the stretching vibrations of $\text{C}=\text{O}$ group.

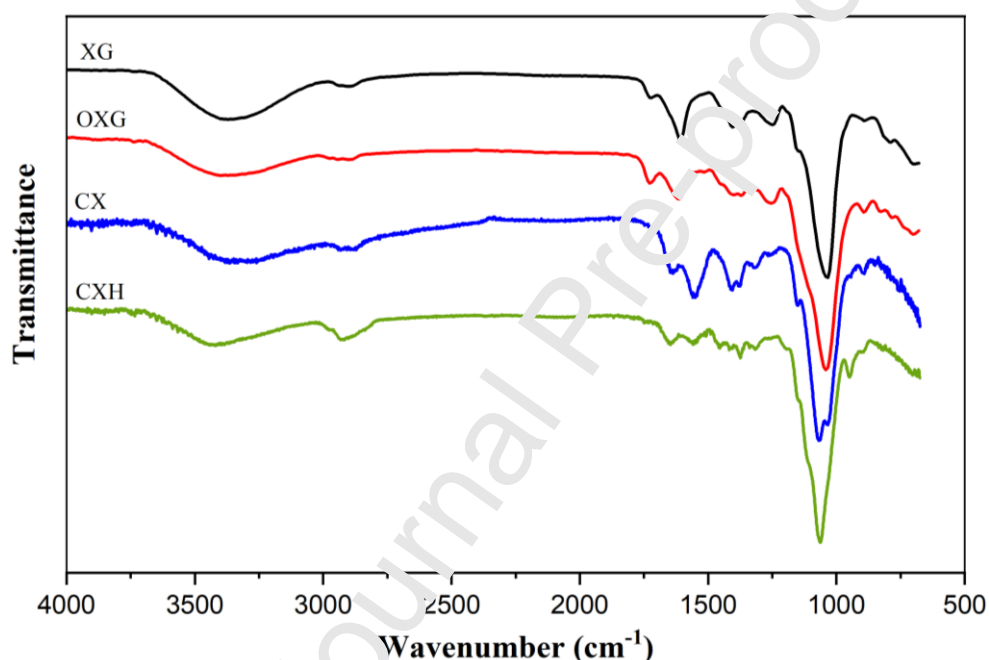


Fig. 3. FTIR spectra of XG, OXG and prepared hydrogel.

3.3.2. Thermogravimetric analysis

Thermogravimetric analysis (TGA) curves for CX and CXH hydrogels are shown in **Fig. 4a**. All thermograms exhibited similar profile and depicted two main stages of weight loss. While the corresponding derivative thermograms (DTG) presented in **Fig. 4b** were used to obtain the onset peak temperature, final peak temperature and the temperature of maximum rate of weight loss. According to the presented thermograms in **Fig. 4**, the first phase weight loss for CX that starts from temperature 30 to $150\text{ }^\circ\text{C}$ was due to the loss of adsorbed and bound water. The second weight loss that starts above $160\text{ }^\circ\text{C}$ with DTG_{max} at $255\text{ }^\circ\text{C}$ was related to the decomposition CX hydrogel major structure. Whereas in the developed CXH hydrogel, an

initial weight loss was observed in the temperature range between 30 to 180 °C. Later decomposition phase began at 200 °C and continued up to 415 °C, which is attributed to the decomposition of the polysaccharide main chains and crosslinked polymeric network. It is obvious that the initial decomposition temperature for CX hydrogel with DTG_{max} at 255 °C is far lower than that observed for CXH (DTG_{max} at 348 °C). This indicates that CX hydrogel was thermally less stable than CXH. This may be attributed to the incorporation of HC in the hydrogel network the drastically enhanced the thermal stability of CXH hydrogel.

3.3.3. Surface morphology analysis

Fig. 4c depicts the surface morphology of the hydrogels examined by SEM. The images showed changes on the surface morphology between the two tested hydrogel samples (CX and CXH). It was obvious from the microphotographs that the surface of the hydrogels were porous. By incorporating HC into the hydrogel, the surface structure of CXH hydrogel displayed a fibrous and dense porous network. This indicates that HC increase intermolecular hydrogen bonds and hydrophilicity of the CXH hydrogel, which in tend increased porosity density in the hydrogel assembly [33]. In addition, the dense network structure may be attributed to the enhanced entanglement of HC in the crosslinked CS-OXG network giving the hydrogels spongy texture. Such porous architecture and connectivity in the developed hydrogel proves highly beneficial and plays an important role in its swelling. This facilitates the entrapment, transport and ultimately release of incorporated bioactive substances [48]. Also by freeze-drying, the process might have contributed to pore size distribution in the hydrogel during drying thereby influencing the preservation of the porous structure [49].

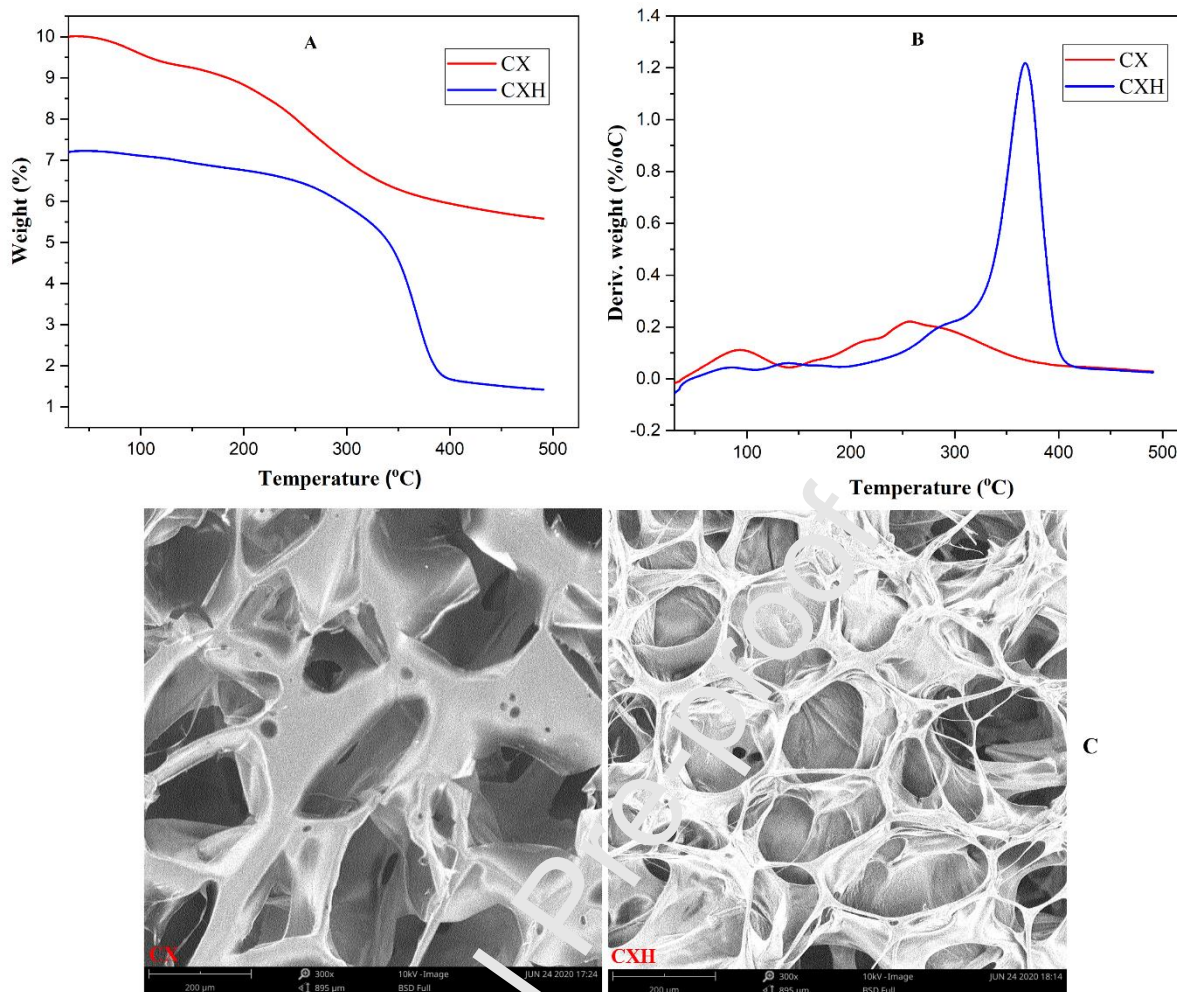


Fig. 4. a) TGA, b) DTG and c) SEM images of prepared CX and CXH hydrogels.

3.3.4. Compression and rheological analysis

Results of unconfined compression testing of CX and CXH hydrogel scaffolds are shown in **Fig. 5a**. According to determined results, CXH hydrogel depicted higher compressive strength compared to CX. In addition, evaluation of compressive modulus of elasticity via the stress-strain profile under 90% compression showed that CXH scaffolds were ≈ 2.0 times less stiff than CX. The optimum compressive modulus at break were determined as 23.56 ± 1.17 and 62.45 ± 3.12 kPa for CX and CXH hydrogels, respectively.

Rheological experiments were also performed to determine the mechanical stability of CX and CXH hydrogels. The storage modulus (G') and loss modulus (G'') were measured as a function of angular frequency (0.1–100 1/s) at constant a strain of 0.1%. As depicted in **Fig. 5b**, the G' values were greater than G'' indicating that the prepared hydrogels are elastic nature. In addition, the mechanical properties of the hydrogels dependent on the composition of the polymer matrix. Overall, CX exhibited weak mechanical properties as compared to

CXH hydrogel. Maximum deformation revealed that the G' values for CX and CXH hydrogels were determined as ≈ 5080 Pa and ≈ 6250 Pa, respectively. The higher strength observed in CXH gel may have been due to the dense structure of the hydrogel, which represents homogeneous miscibility of HC in the crosslinked CS-OXG network.

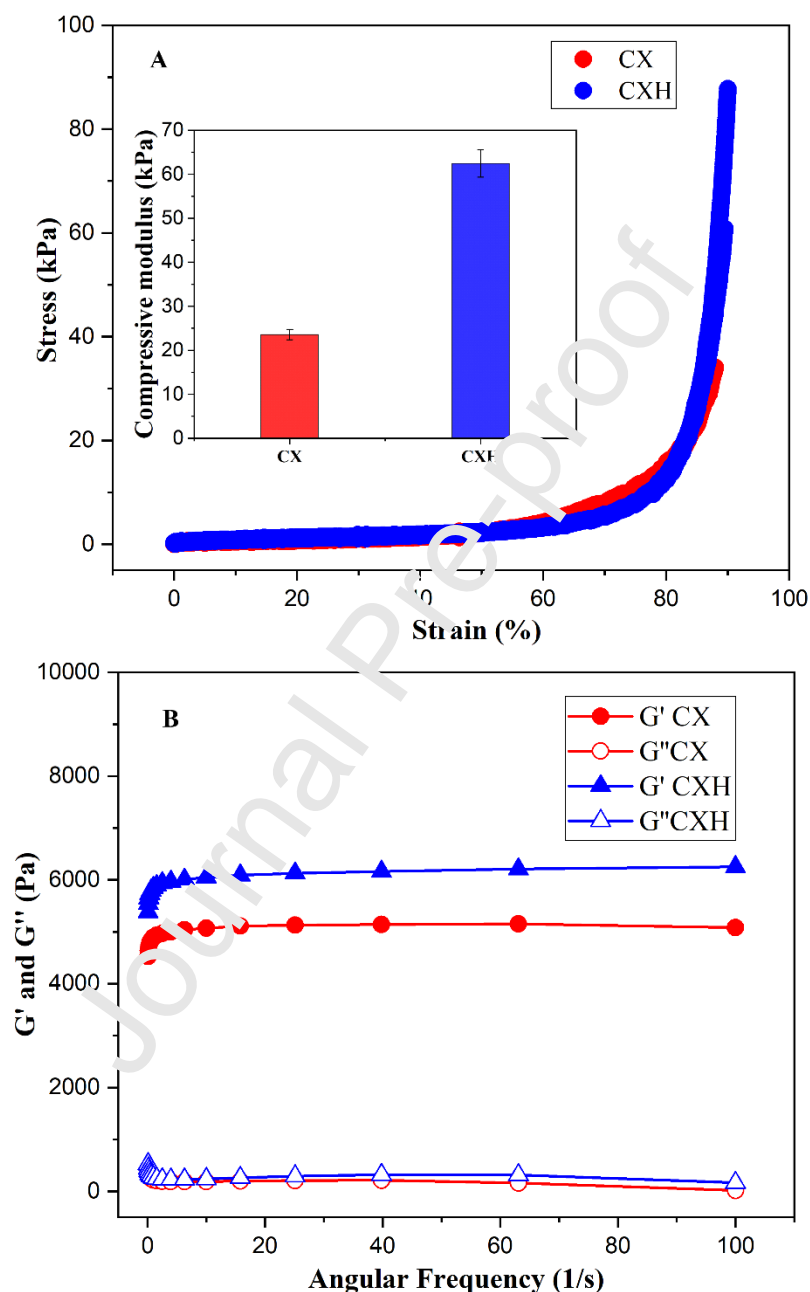


Fig. 5. a) Compressive and b) rheological measurements based on frequency sweep test on wet CX and CXH hydrogels at 25 °C.

3.4. Drug release and kinetics

Biopolymeric hydrogels have been widely used in drug delivery applications since they offer great promise by virtue of biocompatibility, absorbability and swelling properties. Such gel

networks especially when semi-interpenetrated presents more efficiency as drug delivery systems considering it support effective loading of any given drug molecule especially antibiotics [50]. Keeping this in mind, three commonly used therapeutic antibiotic drugs namely ampicillin trihydrate (AT), minocycline hydrochloride (MH) and rifampicin (RC) were selected and investigated as antibacterial drugs in the present study. In general, AT is used to treat bacterial infections such as respiratory tract infections, urinary tract infections, meningitis, salmonellosis, and endocarditis. While MH a tetracycline antibiotic is used to treat infections such as pneumonia and RC is mainly used as a therapeutic agent against infections such as *Mycobacterium avium* complex, leprosy, tuberculosis and Legionnaires' disease [51, 52]. Herein, these selected drugs were investigated for their loading and release efficiency from designed CXH hydrogels. For the investigated loaded samples, maximum DLE% was determined as $93.62 \pm 11.86\%$, $90.86 \pm 0.92\%$ and $34.80 \pm 1.09\%$ for AT, MH and RC drugs, respectively. CDR% of the different drugs as a function of time at SGF pH 2.0 and SIF pH 7.4 are presented in **Fig. 6a** and **b**. Results showed initial burst release in the range of 18-36% within the first 6 h while a sustained release $\geq 50\%$ was achieved after 48 h for all investigated samples. In addition, higher drug release was observed for gel samples in SGF pH 2.0 compared to those in SIF pH 7.4. The higher release may be attributed to the fast and high swelling of the hydrogel which is promoted by the protonation of free amine groups on the backbone of chitosan. The enhanced swelling in acidic medium significant increases the pore sizes in the gel structure thereby leading to rapid release of the drug molecules from the hydrogel network [53]. Maximum cumulative release for all investigated antibiotic drugs in SGF and SIF was reached after 240 h with CDR% greater than 80%. Overall, the porous nature of the freeze-dried hydrogels significantly improved the release rate of the drugs. This exhibits a direct structure-function correlation between hydrogel morphology and antibiotic release as supported by the SEM results.

The drug release experimental data were further fitted to Korsmeyer-Peppas kinetic model best describe the release mechanisms of AT, MH and RC from CXH hydrogel in SGF pH 2.0 and SIF pH 7.4 solutions. The corresponding determined parameters of the model for the linear fitted relationship between the drug release rate and time are provided in **Table 2**. The calculated values of the diffusion exponent (n) at SGF pH 2.0 and SIF pH 7.4 are lesser than 0.5 for all drug-loaded hydrogels. This indicates that the release of the different drugs from CXH hydrogel was majorly dominated by Fickian diffusion mechanism. This diffusion mechanism generally occurs via swelling or disintegration of the polymeric network as well

as diffusion through the polymer matrix [54]. The combination of these different phenomena results in the controlled release of the different drugs from CXH hydrogel. In addition, **Table 2** shows the error analysis parameters of calculated coefficient of determination (R^2), sum squared of errors (SSE), standard deviation of the residuals (SD) and reduced chi-square (χ^2). As observed, the calculated values of CXH loaded drug samples (AT, MH and RC) in both SGF pH 2.0 and SIF pH 7.4 are significantly low and in close agreement to each other. This confirmed that the release kinetics of the different antibiotic drugs from the CXH hydrogel well fitted Korsmeyer-Peppas model.

Table 2

Data of kinetic models for the release of the different drug from CXH hydrogel.

Model parameters	CXH-AT		CXH-MH		CXH-RC	
	pH 2.0	pH 7.4	pH 2.0	pH 7.4	pH 2.0	pH 7.4
<i>Korsmeyer-Peppas</i>						
K_{KP}	8.91	8.57	8.66	8.36	8.35	8.11
n	0.191	0.285	0.267	0.331	0.344	0.400
R^2	0.909	0.983	0.912	0.981	0.922	0.969
SSE	0.0033	0.0013	0.0067	0.0019	0.0091	0.0045
χ^2	1.09×10^{-3}	4.22×10^{-4}	2.07×10^{-3}	6.28×10^{-4}	3.02×10^{-3}	1.51×10^{-3}
SD	0.033	0.021	0.046	0.025	0.055	0.039

3.5. *In vitro* biological assay and degradation of gels

In the design of new hydrogel scaffolds as suitable drug carriers for delivery at targeted sites, the cytotoxicity of its constituents is vital. For this reason, MTT test was performed and the viability of cells in the drug loaded hydrogels of CXH-AT, CXH-MH and CXH-RC were determined and compared to non-loaded CXH as control (**Fig. 6c**). The viability of cells exposed to extracts of CXH loaded hydrogels were assayed as 86.77, 81.73 and 87.09% for CXH-AT, CXH-MH and CXH-RC, respectively, compared to CXH that was obtained as 95.68%. These results obtained for the loaded samples are not significantly different when compared to the control. This suggests that the extracts of the drug loaded hydrogels can enhance cell proliferation when compared to the control sample. The low cell cytotoxicity of the prepared hydrogels can be attributed to the biocompatibility and hydrophilicity of the polymers used. This creates a suitable and facile method for the synthesis of sterile scaffolds suitable for drug delivery and tissue regeneration application.

Fig. 6d shows the degradation rate of CXH hydrogels at 37 °C in PBS pH 7.4 within a period of 30 days. As observed, the weight loss of CXH hydrogel gradually increases as a function of time. However, less than 50% degradation was achieved within 30 days with maximum

weight loss determined as $37.48 \pm 1.87\%$. This low degradation could be due to high intra/inter molecular and polymer chain interaction between the different polymer moieties leading to a stable and homogenous structural network complex of crosslinked CS-OXG interpenetrated with HC.

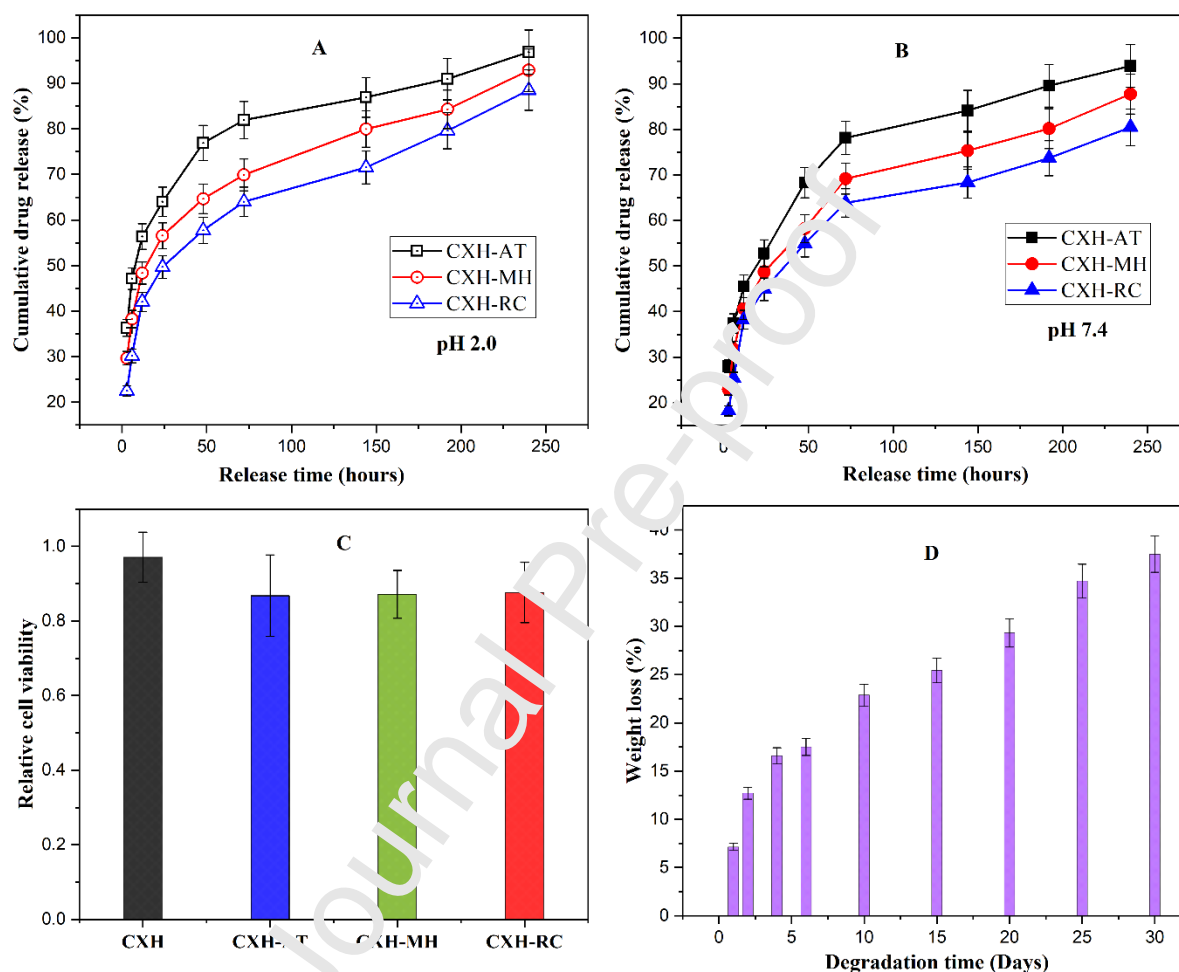


Fig. 6. Cumulative release of ampicillin trihydrate (AT), minocycline hydrochloride (MH) and rifampicin (RC) from CXH hydrogel at 37 °C in PBS a) pH 2.0 and b) pH 7.4. c) Cytotoxicity assay of non-loaded (CXH) and antibiotic loaded (CXH-AT, CXH-MH, and CXH-RC) hydrogel scaffolds. Cell seeding concentration at 1×10^5 cells/mL. d) *In vitro* degradation of CXH gel as a function of time.

3.6. Antibacterial activity of gels

The prepared drug loaded hydrogels (CXH-AT, CXH-MH and CXH-RC) were exposed to *E. coli*, *S. aureus* and *K. pneumonia* bacterial suspensions to evaluate their antibacterial activities (**Fig. 7**). The hydrogels were placed into petri dishes containing the culture medium and then incubated at 37 °C for 18 h to determine the growth inhibition of bacterial cells. The

inhibition zones were measured and the results are presented in **Table 3**. According to obtained results, the drug loaded hydrogels showed high antibacterial action compared to the control samples with minimal inhibition. The low inhibition from control samples may be attributed to the antibacterial property of chitosan. However, the highest inhibition zones for the different bacteria investigated was observed for *S. aureus*. Overall, high antibacterial action was achieved for all the different antibiotic drugs loaded into CXH hydrogel.

Table 3
Inhibition zones of CXH hydrogels.

Samples	Diameter of inhibition zones (mm)		
	<i>S.aureus</i> (G+)	<i>E.coli</i> (G-)	<i>K. pneumoniae</i> (G-)
CXH	8.1±0.04	0.6±0.07	1.2±0.13
CXH-AT	42.9±0.29	17.4±0.39	9.1±0.24
CXH-MH	27.7±0.14	17.3±0.41	26.0±0.34
CXH-RC	35.4±0.33	15.5±0.21	15.4±0.22

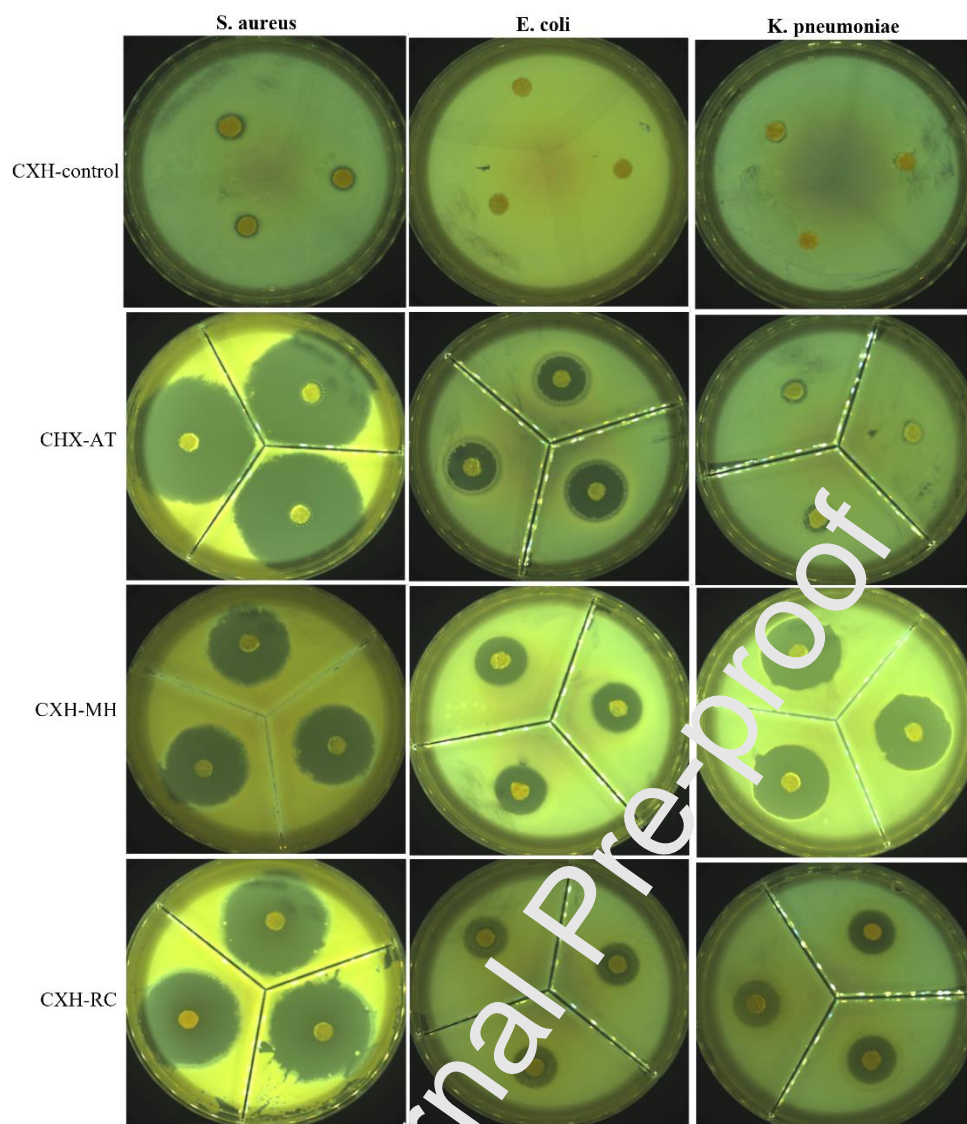


Fig. 7. Illustration of antibacterial action of CXH gels based on inhibition zones.

4. Conclusions

Self-crosslinked chitosan-dialdehyde xanthan gum interpenetrated hydrogels were successfully prepared by mixing with hydroxypropyl methylcellulose. The hydrogels showed good swelling and porosity, flexibility, high thermal stability and high mechanical properties. The mechanical properties of the hydrogels were dependent on the ratio of HC exhibiting high storage and compressive modulus. By increasing the concentration of HC in the initial reaction mixture depicted to improve mechanical and structural stability of the hydrogel scaffolds. The loaded hydrogels with different antibiotic drugs showed high cumulative sustain release percentage of more than 80%. The prepared hydrogels also depicted excellent antibacterial activity against tested Gram-positive and Gram-negative bacteria. These obtained results demonstrated that the developed hydrogel in the present study may emerge

as a suitable drug vehicle for different bioactive molecules. Considering several studies have revealed the biocompatibility and biodegradability capability of biopolymeric based materials, the present hydrogel system shows promising application in drug delivery and tissue regeneration.

CRedit author statement

Fahanwi Asabuwa Ngwabebhoh: Conceptualization, Methodology, Investigation and Writing-original draft preparation. **Oyunchimeg Zandraa:** Methodology and Formal analysis. **Rahul Patwa:** Formal analysis and Data curation. **Zdenka Capáková:** Formal analysis and Data curation. **Nabanita Saha:** Supervision, Reviewing and Editing. **Petr Saha:** Supervision and Funding acquisition.

Declaration of competing interest

The authors declare no competing financial interest.

Acknowledgements

The authors acknowledge the support of this work by Tomas Bata University in Zlin and the Ministry of Education, Youth & Sports of the Czech Republic - DKRVO (RP/CPS/2020/005) for the financial support of this work.

References

- [1] Y. Zhao, X. Zhang, Y. Wang, Z. Wu, J. An, Z. Lu, L. Mei, C. Li, In situ cross-linked polysaccharide hydrogel as extracellular matrix mimics for antibiotics delivery, *Carbohydrate Polymers* 105 (2014) 63-69.
- [2] B. Singh, V. Sharma, Design of psyllium–PVA–acrylic acid based novel hydrogels for use in antibiotic drug delivery, *International Journal of Pharmaceutics* 389(1) (2010) 94-106.
- [3] L. Yang, C. Zhang, F. Huang, J. Liu, Y. Zhang, C. Yang, C. Ren, L. Chu, B. Liu, J. Liu, Triclosan-based supramolecular hydrogels as nanoantibiotics for enhanced antibacterial activity, *Journal of Controlled Release* 324 (2020) 354-365.
- [4] J. Chotitumnavee, T. Parakaw, R.L. Srisatjaluk, C. Pruksaniyom, S. Pisitpipattana, C. Thanathipanont, T. Amarasinh, N. Tiankhum, N. Chimchawee, N. Ruangsawasdi, In vitro evaluation of local antibiotic delivery via fibrin hydrogel, *J. Dental Sci.* 14(1) (2019) 7-14.
- [5] P. Kaur, V.S. Gondil, S. Chhibber, A novel wound dressing consisting of PVA-SA hybrid hydrogel membrane for topical delivery of bacteriophages and antibiotics, *International Journal of Pharmaceutics* 572 (2019) 13.

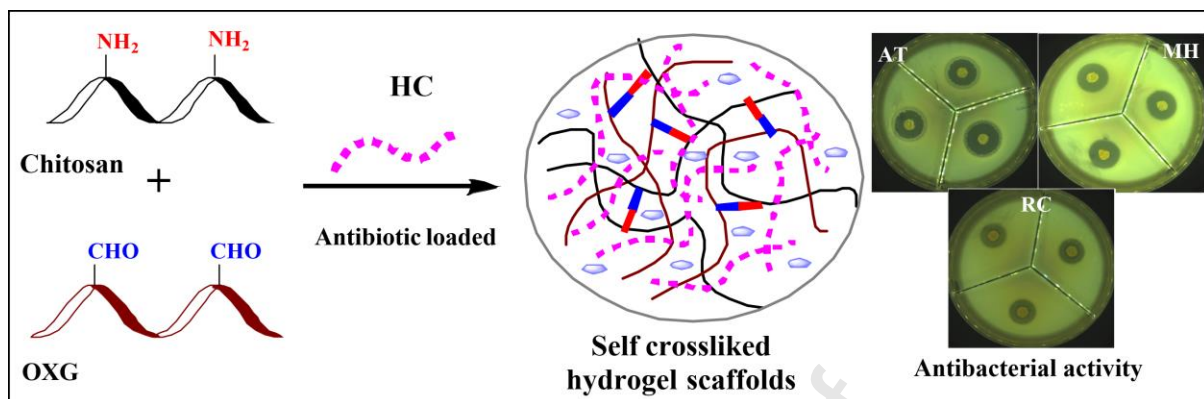
- [6] J. Wroblewska-Krepsztul, T. Rydzkowski, I. Michalska-Pozoga, V.K. Thakur, *Biopolymers for Biomedical and Pharmaceutical Applications: Recent Advances and Overview of Alginate Electrospinning*, *Nanomaterials* 9(3) (2019).
- [7] K. Dharmalingam, R. Anandalakshmi, Fabrication, characterization and drug loading efficiency of citric acid crosslinked NaCMC-HPMC hydrogel films for wound healing drug delivery applications, *International Journal of Biological Macromolecules* 134 (2019) 815-829.
- [8] L.P. Cao, B. Cao, C.J. Lu, G.W. Wang, L. Yu, J.D. Ding, An injectable hydrogel formed by in situ cross-linking of glycol chitosan and multi-benzaldehyde functionalized PEG analogues for cartilage tissue engineering, *Journal of Materials Chemistry B* 3(7) (2015) 1268-1280.
- [9] S.I. Erdagi, F.A. Ngwabebhoh, U. Yildiz, Genipin crosslinked gelatin-diosgenin-nanocellulose hydrogels for potential wound dressing and healing applications, *International Journal of Biological Macromolecules* 149 (2020), 551-663.
- [10] W.S. Toh, X.J. Loh, Advances in hydrogel delivery systems for tissue regeneration, *Materials Science and Engineering: C* 45 (2014) 690-697.
- [11] A.M. George, S.P.R. Peddireddy, G. Thakur, F.C. Rodrigues, *Biopolymer-based scaffolds: Development and biomedical application*, *Biopolymer-Based Formulations*, Elsevier2020, pp. 717-749.
- [12] S. Van Vlierberghe, P. Dubruel, E. Schacht, *Biopolymer-based hydrogels as scaffolds for tissue engineering applications: a review*, *Biomacromolecules* 12(5) (2011) 1387-1408.
- [13] S. Atta, S. Khaliq, A. Islam, I. Javeri, T. Jamil, M.M. Athar, M.I. Shafiq, A. Ghaffar, *Injectable biopolymer based hydrogels for drug delivery applications*, *International journal of biological macromolecules* 80 (2015) 240-245.
- [14] B. Kaczmarek, K. Nadolna, A. Owczarek, *The physical and chemical properties of hydrogels based on natural polymers*, *Hydrogels Based on Natural Polymers*, Elsevier2020, pp. 151-172.
- [15] Z. Bao, C. Xian, Q. Yuan, G. Liu, J. Wu, *Natural Polymer- Based Hydrogels with Enhanced Mechanical Performances: Preparation, Structure, and Property*, *Advanced healthcare materials* 8(17) (2019) 1900670.
- [16] M.N.R. Kumar, *A review of chitin and chitosan applications*, *Reactive and functional polymers* 46(1) (2000) 1-27.
- [17] N. Bhattarai, J. Gunn, M. Zhang, *Chitosan-based hydrogels for controlled, localized drug delivery*, *Advanced drug delivery reviews* 62(1) (2010) 83-99.
- [18] A. Shalviri, Q. Liu, M.J. Abdekhodaie, X.Y. Wu, *Novel modified starch-xanthan gum hydrogels for controlled drug delivery: Synthesis and characterization*, *Carbohydrate Polymers* 79(4) (2010) 898-907.
- [19] J. Guo, L. Ge, X. Li, C. Mu, D. Li, *Periodate oxidation of xanthan gum and its crosslinking effects on gelatin-based edible films*, *Food Hydrocolloids* 39 (2014) 243-250.
- [20] E.A. Kamoun, *N-succinyl chitosan-dialdehyde starch hybrid hydrogels for biomedical applications*, *Journal of Advanced research* 7(1) (2016) 69-77.

- [21] D. Li, Y. Ye, D. Li, X. Li, C. Mu, Biological properties of dialdehyde carboxymethyl cellulose crosslinked gelatin-PEG composite hydrogel fibers for wound dressings, *Carbohydrate polymers* 137 (2016) 508-514.
- [22] Y. Gong, G. Liu, W. Peng, X. Su, J. Chen, Immobilization of the proteins in the natural rubber with dialdehyde sodium alginate, *Carbohydrate polymers* 98(2) (2013) 1360-1365.
- [23] M.M. Ibrahim, A. Koschella, G. Kadry, T. Heinze, Evaluation of cellulose and carboxymethyl cellulose/poly (vinyl alcohol) membranes, *Carbohydrate polymers* 95(1) (2013) 414-420.
- [24] J. Siepmann, N. Peppas, Modeling of drug release from delivery systems based on hydroxypropyl methylcellulose (HPMC), *Advanced drug delivery reviews* 64 (2012) 163-174.
- [25] A. Mujtaba, K. Kohli, In vitro/in vivo evaluation of HPMC/alginate based extended-release matrix tablets of cefpodoxime proxetil, *International Journal of Biological Macromolecules* 89 (2016) 434-441.
- [26] L.M. Ge, X.Y. Li, R. Zhang, T.H. Yang, X.W. Ye, D.F. Li, C.D. Mu, Development and characterization of dialdehyde xanthan gum crosslinked gelatin based edible films incorporated with amino-functionalized montmorillonite, *Food Hydrocolloids* 51 (2015) 129-135.
- [27] Y. Zuo, W. Liu, J. Xiao, X. Zhao, Y. Zhu, Y. Wu, Preparation and characterization of dialdehyde starch by one-step acid hydrolysis and oxidation, *International Journal of Biological Macromolecules* 103 (2017) 1237-1254.
- [28] B.T. Hofreiter, B.H. Alexander, I.A. Wolf, Rapid estimation of dialdehyde content of periodate oxystarch through quantitative alkali consumption, *Analytical Chemistry* 27(12) (1955) 1930-1931.
- [29] G.T. Hermanson, *Bioconjugate techniques*, Academic press 2013.
- [30] F. Ganji, M.J. Abdekhodaie, A. Ramazani S.A, Gelation time and degradation rate of chitosan-based injectable hydrogel, *Journal of Sol-Gel Science and Technology* 42(1) (2007) 47-53.
- [31] D. Gupta, C.H. Tator, M.S. Shoichet, Fast-gelling injectable blend of hyaluronan and methylcellulose for intrathecal, localized delivery to the injured spinal cord, *Biomaterials* 27(11) (2006) 2370-2376.
- [32] M. Pandey, N. Mohamad, M.C.I.M. Amin, Bacterial cellulose/acrylamide pH-sensitive smart hydrogel: development, characterization, and toxicity studies in ICR mice model, *Molecular pharmaceutics* 11(10) (2014) 3596-3608.
- [33] N.S. Malik, M. Ahmad, M.U. Minhas, R. Tulain, K. Barkat, I. Khalid, Q. Khalid, Chitosan/Xanthan Gum Based Hydrogels as Potential Carrier for an Antiviral Drug: Fabrication, Characterization, and Safety Evaluation, *Frontiers in Chemistry* 8(50) (2020).
- [34] S. Kaur, M. Garg, S. Mittal, N. Wangoo, R.K.J.S. Sharma, A.B. Chemical, Copper based facile, sensitive and low cost colorimetric assay for ampicillin sensing and quantification in nano delivery system, 248 (2017) 234-239.
- [35] J. Siepmann, N.A. Peppas, Modeling of drug release from delivery systems based on hydroxypropyl methylcellulose (HPMC), *Advanced Drug Delivery Reviews* 64 (2012) 163-174.

- [36] Y. Gao, J. Zuo, N. Bou-Chacra, T.d.J.A. Pinto, S.-D. Clas, R.B. Walker, R. Löbenberg, In vitro release kinetics of antituberculosis drugs from nanoparticles assessed using a modified dissolution apparatus, *Biomed Res. Int.* 2013 (2013) 136590-136590.
- [37] X. Ma, T. Xu, W. Chen, H. Qin, B. Chi, Z. Ye, Injectable hydrogels based on the hyaluronic acid and poly (γ -glutamic acid) for controlled protein delivery, *Carbohydrate Polymers* 179 (2018) 100-109.
- [38] M. Fan, Y. Ma, H. Tan, Y. Jia, S. Zou, S. Guo, M. Zhao, H. Huang, Z. Ling, Y. Chen, X. Hu, Covalent and injectable chitosan-chondroitin sulfate hydrogels embedded with chitosan microspheres for drug delivery and tissue engineering, *Materials Science and Engineering: C* 71 (2017) 67-74.
- [39] C. Mu, J. Guo, X. Li, W. Lin, D. Li, Preparation and properties of dialdehyde carboxymethyl cellulose crosslinked gelatin edible films, *Food Hydrocolloids* 27(1) (2012) 22-29.
- [40] Z. Emami, M. Ehsani, M. Zandi, R. Foudazi, Controlling alginate oxidation conditions for making alginate-gelatin hydrogels, *Carbohydrate Polymers* 198 (2018) 509-517.
- [41] A. Potthast, T. Rosenau, P. Kosma, Analysis of oxidized functionalities in cellulose, *Polysaccharides ii*, Springer 2006, pp. 1-48.
- [42] L. Zhang, J. Liu, X. Zheng, A. Zhang, X. Zhang, K. Tang, Pullulan dialdehyde crosslinked gelatin hydrogels with high strength for biomedical applications, *Carbohydrate Polymers* 216 (2019) 45-53.
- [43] N.S. Malik, M. Ahmad, M.U. Minhas, R. Gulain, K. Barkat, I. Khalid, Q. Khalid, Chitosan/Xanthan Gum Based Hydrogels as Potential Carrier for an Antiviral Drug: Fabrication, Characterization, and Safety Evaluation, *Frontiers in Chemistry* 8 (2020) 50.
- [44] S.C. Barros, A.A. da Silva, D.B. Costa, I. Cesarino, C.M. Costa, S. Lanceros-Méndez, A. Pawlicka, M.M. Silva, Thermally sensitive chitosan-cellulose derivative hydrogels: swelling behaviour and morphologic studies, *Cellulose* 21(6) (2014) 4531-4544.
- [45] G. Tejada, G. Piccirilli, M. Sortino, C. Salomón, M. Lamas, D. Leonardi, Formulation and in-vitro efficacy of antifungal mucoadhesive polymeric matrices for the delivery of miconazole nitrate, *Materials Science and Engineering: C* 79 (2017) 140-150.
- [46] N.L. Calvo, L.A. Sveta, V.A. Alvarez, A.D. Quiroga, M.C. Lamas, D. Leonardi, Chitosan-hydroxypropyl methylcellulose tioconazole films: A promising alternative dosage form for the treatment of vaginal candidiasis, *International Journal of Pharmaceutics* 556 (2019) 181-191.
- [47] C. Ding, M. Zhang, G. Li, Preparation and characterization of collagen/hydroxypropyl methylcellulose (HPMC) blend film, *Carbohydrate polymers* 119 (2015) 194-201.
- [48] I. Khalid, M. Ahmad, M. Usman Minhas, K. Barkat, Synthesis and evaluation of chondroitin sulfate based hydrogels of loxoprofen with adjustable properties as controlled release carriers, *Carbohydrate Polymers* 181 (2018) 1169-1179.
- [49] K. Kabiri, M. Zohuriaan- Mehr, Porous superabsorbent hydrogel composites: synthesis, morphology and swelling rate, *Macromolecular Materials and Engineering* 289(7) (2004) 653-661.
- [50] T. Chandy, C.P. Sharma, Chitosan matrix for oral sustained delivery of ampicillin, *Biomaterials* 14(12) (1993) 939-944.

- [51] P. Singh, P. Manhas, R. Sharma, S.K. Pandey, R.K. Sharma, O.P. Katare, N. Wangoo, Self-assembled dipeptide nanospheres as single component based delivery vehicle for ampicillin and doxorubicin, *Journal of Molecular Liquids* 312 (2020) 113420.
- [52] Z. Nazemi, M.S. Nourbakhsh, S. Kiani, Y. Heydari, M.K. Ashtiani, H. Daemi, H. Baharvand, Co-delivery of minocycline and paclitaxel from injectable hydrogel for treatment of spinal cord injury, *Journal of Controlled Release* 321 (2020) 145-158.
- [53] M.V. Risbud, A.A. Hardikar, S.V. Bhat, R.R. Bhonde, pH-sensitive freeze-dried chitosan-polyvinyl pyrrolidone hydrogels as controlled release system for antibiotic delivery, *Journal of Controlled Release* 68(1) (2000) 23-30.
- [54] T.N.d. Silva, F. Reynaud, P.H.d.S. Picciani, K.G. de Holanda e Silva, T.N. Barradas, Chitosan-based films containing nanoemulsions of methyl salicylate: Formulation development, physical-chemical and in vitro drug release characterization, *International Journal of Biological Macromolecules* 164 (2020) 2558-2568.

Graphical abstract



Research highlights

- ✓ Self-crosslinked chitosan/xanthan interpenetrated hypromellose hydrogels were developed.
- ✓ Hydrogels showed good mechanical stability and high pore distribution.
- ✓ The hydrogel scaffolds were loaded with ampicillin, minocycline and rifampicin drugs.
- ✓ The scaffolds showed good *in vitro* release, biocompatibility and antibacterial activity.

Journal Pre-proof